THE JOURNAL OF BIOLOGICAL CHEMISTRY VOL. 285, NO. 12, pp. 8995–9007, March 19, 2010
Printed in the U.S.A.

Substrate Specificity, Membrane Topology, and Activity Regulation of Human Alkaline Ceramidase 2 (ACER2)*

Received for publication, September 22, 2009, and in revised form, January 14, 2010 Published, JBC Papers in Press, January 20, 2010, DOI 10.1074/jbc.M109.069203

Wei Sun[‡1], Junfei Jin[‡1], Ruijuan Xu[‡1], Wei Hu[‡], Zdzislaw M. Szulc[§], Jacek Bielawski[§], Lina M. Obeid[‡§¶], and Cungui Mao[‡§2]

From the Departments of [‡]Medicine and [§]Biochemistry and Molecular Biology and the [¶]Ralph H. Johnson Veterans Affairs Hospital, Medical University of South Carolina, Charleston, South Carolina 29425

Human alkaline ceramidase 2 (ACER2) plays an important role in cellular responses by regulating the hydrolysis of ceramides in cells. Here we report its biochemical characterization, membrane topology, and activity regulation. Recombinant ACER2 was expressed in yeast mutant cells (Δ*ypc1*Δ*ydc1*) that lack endogenous ceramidase activity, and microsomes from ACER2-expressiong yeast cells were used to biochemically characterize ACER2. ACER2 catalyzed the hydrolysis of various ceramides and followed Michaelis-Menten kinetics. ACER2 required Ca^{2+} for both its *in vitro* and cellular activities. ACER2 has 7 putative transmembrane domains, and its amino (N) and carboxyl (C) termini were found to be oriented in the lumen of the Golgi complex and cytosol, respectively. ACER2 mutant (ACER2ΔN36) lacking the N-terminal tail (the first 36 amino acid residues) exhibited undetectable activity and was mislocalized to the endoplasmic reticulum, suggesting that the N-terminal tail is necessary for both ACER2 activity and Golgi localization. ACER2 mutant (ACER2ΔN13) lacking the first 13 residues was also mislocalized to the endoplasmic reticulum although it retained ceramidase activity. Overexpression of ACER2, ACER2ΔN13, but not ACER2ΔN36 increased the release of sphingosine 1-phosphate from cells, suggesting that its mislocalization does not affect the ability of ACER2 to regulate sphingosine 1-phosphate secretion. However, overexpression of ACER2 but not ACER2ΔN13 or ACER2ΔN36 inhibited the glycosylation of integrin β1 subunit and Lamp1, suggesting that its mistargeting abolishes the ability of ACER2 to regulation protein glycosylation. These data suggest that ACER2 has broad substrate specificity and requires Ca^{2+} for its activity and that ACER2 has the cytosolic C terminus and luminal N terminus, which are essential for its activity, correct cellular localization, and regulation for protein glycosylation.

Ceramidases are enzymes that catalyze the hydrolysis of ceramides to form SPH[3] (1), which in turn, is phosphorylated to form sphingosine 1-phosphate (S1P) (2). Ceramide, SPH, and S1P are bioactive lipids that mediate various cellular responses. Both ceramides and SPH have been shown to induce cell growth arrest, differentiation, and apoptosis (3, 4). In contrast, S1P mainly promotes cell proliferation and survival (5). Due to the opposing role of ceramide and SPH *versus* S1P in cell survival and proliferation, it has been suggested that the balance between ceramide/SPH and S1P levels may determine the fate of the cell to proliferate and live or to undergo growth arrest and die (5). Therefore, as key enzymes that regulate the metabolism of these bioactive lipids, ceramidases may play an important role in cell fate decision.

ACER2 is one of three human alkaline ceramidases that we recently cloned (6). We demonstrated by Northern blot and quantitative PCR that ACER2 mRNA is expressed highly in the placenta but moderately in other tissues (6). ACER2 is a Golgi membrane protein with several putative transmembrane domains (TMDs) (6). Moderate ectopic expression of ACER2 promotes cell proliferation and survival probably by decreasing levels of ceramides while elevating levels of S1P (6). Interestingly, high ectopic expression of ACER2 causes fragmentation of the Golgi complex and inhibits cell proliferation due to an aberrant increase in the cellular levels of SPH (6). These results suggest that ACER2 is actively involved in cell fate decisions by controlling the relative levels of ceramides, SPH, and S1P. In addition to cell growth and survival, our recent studies demonstrated that ACER2 has an important role in regulating protein glycosylation in the Golgi complex (7). ACER2 overexpression inhibits the glycosylation of the precursor of the integrin β1 subunit (β1), resulting in an inhibition of β1 integrin-mediated cell adhesion to extracellular matrices. In contrast, ACER2 down-regulation by RNA interference enhances the glycosylation of the integrin β1 subunit, thus promoting cell adhesion. We also demonstrated that ACER2 expression is up-regulated in cells by serum deprivation (6) or all-*trans*-retinoic acid (7) but down-regulated by the tumor promoter phorbol 12-myristate 13-acetate (7), suggesting that ACER2 is a highly regulated protein.

Although ACER2 plays such an important role in cellular responses, much remains unknown about its biochemical prop-

* This work was supported, in whole or in part, by National Institutes of Health Grant R01CA104834 (to C. M.) and a Veterans Affairs Merit award (to L. M. O.).

[1] These authors contributed equally to this work.

[2] To whom correspondence should be addressed: Division of General Internal Medicine, Dept. of Medicine, 114 Doughty St., Rm. 646, STB, P. O. Box 250779, Charleston, SC 29425. Tel.: 843-876-5173; Fax: 843-876-5172; E-mail: maoc@musc.edu.

[3] The abbreviations used are: SPH, sphingosine; S1P, sphingosine 1-phosphate; ESI/MS, electrospray ionization-mass spectrometric analysis; DMSO, dimethyl sulfoxide; ACER2, alkaline ceramidase 2; TMD, transmembrane domain; MEM, minimal essential medium; PBS, phosphate-buffered saline; BSA, bovine serum albumin; FITC, fluorescein isothiocyanate; HPLC, high pressure liquid chromatography; Pipes, 1,4-piperazinediethanesulfonic acid; TET, tetracycline; BAPTA-AM, 1,2-bis(2-aminophenoxyl)ethane-*N*,*N*,*N*′,*N*′-tetraacetic acid acetoxy methyl ester; ER, endoplasmic reticulum; THAP, thapsigargin.

erties, membrane topology, and activity regulation. In this study, we show that ACER2 uses various ceramide species as substrates and that it requires Ca^{2+} for both its *in vitro* and cellular activity. We also find that the amino (N) terminus and carboxyl (C) terminus are oriented in the lumen of the Golgi complex and cytosol, respectively, and that the N-terminal tail is required for both ACER2 activity and Golgi localization. Finally, we demonstrate that its localization to the Golgi complex is essential for ACER2 to regulate protein glycosylation in the Golgi complex. Thus, this study not only reveals biochemical properties and membrane topology of ACER2 but also identifies Ca^{2+} in the lumen of the Golgi complex as a key regulator of the metabolism of sphingolipids.

EXPERIMENTAL PROCEDURES

Reagents—The anti-ACER2 antibody was previously raised against a peptide located at the C terminus of ACER2 in our laboratory (6). Anti-giantin, integrin β1 subunit, calreticulin, Lamp1, and mannosidase antibodies were from Covance (Princeton, NJ), BD Biosciences (San Jose, CA), Sigma, Santa Cruz Biotechnology (Santa Cruz, CA), and Abcam (Cambridge, MA), respectively. *o*-Phthalaldehyde was from FLUKA (Milwaukee, WI). Minimal essential medium (MEM), fetal bovine serum, trypsin-EDTA, Ca^{2+}-free phosphate-buffered saline (PBS), penicillin/streptomycin, Lipofectamine 2000, growth factors (epidermal growth factor, fibroblast growth factor-1, and insulin-like growth factor-1), and Fluo-4 AM were purchased from Invitrogen. Yeast culture medium was from Clontech. D-e-$C_{20:1}$-ceramide and D-e-$C_{20:4}$-ceramide were synthesized in the Lipidomics Core Facility at the Medical University of South Carolina. Other lipids used in this study were purchased from Avanti Polar Lipids. SMEM (a Ca^{2+}-free medium), monoclonal anti-FLAG antibody, and other unlisted chemicals were purchased from Sigma.

Expression of ACER2 and Its Mutants in Mammalian Cells—The ACER2-TET-ON cell line that stably expresses the FLAG-tagged ACER2 (FLAG-ACER2) under the control of the TET-ON promoter system was constructed in our previous study (6). The expression of FLAG-ACER2 in these cells is suppressed in the absence of tetracycline but induced by tetracycline that is added to medium. To transiently express wild-type ACER2 (ACER2), the full-length ACER2 coding sequence plus the FLAG tag sequence was subcloned from pcDNA4-ACER2 to the pcDNA3.1(+) vector (Invitrogen), and the resulting expression construct pcDNA3-ACER2 was obtained. To transiently express the ACER2 mutant (ACER2ΔN13) that lacks the first 13 amino acid residues at the N terminus, the coding sequences lacking the first 45 base pairs at the 5′-end was cloned in-frame with the epitope FLAG tag coding sequence into the vector pcDNA3-FLAG that was constructed in our previous study (8). The ACER2ΔN13 coding sequence was amplified from pcDNA4-FLAG-ACER2 (which was constructed in our previous study (6)) using primers 5′-GGTGATCAGAGGTGGACTGGTGCGAG-3′ (the forward primer, underlined is BclI site) and 5′-CGGAATTCTCACGTGATCTTGACTGATGATTTC-3′ (the reverse primer, underlined is EcoRI site). After being digested with the restriction enzymes BclI and EcoRI, the resulting PCR products were inserted into the BamHI and EcoRI sites of pcDNA3-FLAG. The resulting expression construct pcDNA3-ACER2ΔN13, which directs the expression of the FLAG-tagged ACER2ΔN13, was obtained. The same strategy was applied to obtain the expression construct (pcDNA3-ACER2ΔN36) of the ACER2 mutant (ACER2ΔN36) that lacks the first 36 amino acid residues. The forward PCR primer to amplify the ACER2ΔN36 coding sequence is 5′-GGTGATCAATCAGCAATGTCTTATTTTTCA-3′ (underlined is BclI site), and the reverse primer is the same as that used for the amplification of the coding sequence of ACER2ΔN13. Finally, pcDNA3-FLAG, pcDNA3-ACER2, pcDNA3-ACER2ΔN13, or pcDNA3-ACER2ΔN36 were transiently transfected into HeLa cells using Lipofectamine 2000 as described (6).

ACER2 Expression in Yeast Cells—The FLAG-ACER2 or FLAG-ACER2ΔN36 coding sequence was subcloned into the yeast expression plasmid pYES2 from plasmids pcDNA4-FLAG-ACER2 or pcDNA3-ACER2ΔN36, respectively. The resulting pYES2-FLAG-ACER2 or pYES2-FLAG-ACER2ΔN36 plasmids were transformed into yeast mutant cells (Δ*ypc1*Δ*ydc1*) in which both yeast alkaline ceramidases were deleted (8), and transformants were selected on agar plates containing synthetic defined uracil dropout medium containing dextrose (SD-ura/glu; Clontech). One representative transformant overexpressing FLAG-ACER2 or FLAG-ACER2ΔN36, denoted as Δ*ypc1*Δ*ydc1*ACER2 or Δ*ypc1*Δ*ydc1*ACER2ΔN36 strains, respectively, was chosen for further studies. To express ACER2 or ACER2ΔN36, Δ*ypc1*Δ*ydc1*ACER2 or Δ*ypc1*Δ*ydc1*ACER2ΔN36 cells were grown in SC-ura medium to the stationary phase before being switched to SD-ura medium containing galactose/raffinose (SD-ura/gal; Clontech). After a 10-h culture in SD-ura/gal medium, yeast cells were harvested, and microsomes were prepared as described in our previous studies (8–10).

Immunocytochemistry—Immunocytochemistry was performed essentially as described (11). Briefly, cells were fixed with 3.75% paraformaldehyde buffered with PBS. The fixed cells were permeabilized with 3 μg/ml of digitonin for 10 min at 4 °C or with 0.05% Triton X-100 at room temperature. After being blocked with BSA for 30 min, cells were then incubated for 1 h with primary antibody(s). After washing with PBS, the cells were incubated for 1 h with secondary antibody(s) conjugated with either rhodamine or fluorescein isothiocyanate (FITC). After a final wash with PBS, cells were imaged on a confocal microscope (Zeiss LSM510 Meta).

Protein Concentration Determination—Protein concentrations were determined with BSA as a standard using a BCA protein determination kit (Pierce) according to the manufacturer's instructions.

Western Blot Analysis—Proteins were separated on SDS-polyacrylamide gels and transferred onto nitrocellulose membranes, which were then incubated with various antibodies as described (6).

Lipid Extraction—Total lipids were extracted from cells according to the Bligh-Dyer method (12).

Ceramidase Activity Assay—Ceramidase activity was determined by the release of the long-chain base SPH, from ceramides as described (6). Briefly, a substrate was dispersed into a buffer containing 0.3% Triton X-100 by a water bath sonication.

The lipid/detergent mixture was boiled for 30 s and chilled on ice immediately to form homogeneous lipid/detergent micelles, which were mixed on ice with an equal volume of microsomes suspended in the same buffer but with no Triton X-100. Enzymatic reactions were initiated by incubating the substrate/enzyme mixtures at 37 °C for 20 min. The reactions were stopped by boiling, and an internal standard (D-e-C_{17}-SPH, C17SPH) was added to the reaction mixtures, which were dried at 100 °C in a vacuum oven. The amounts of SPH in the enzymatic reactions were determined as described below. Both reaction time and amount of enzyme were within the linear range.

HPLC Analysis for Sphingoid Bases—SPH or DHS in enzymatic reactions or lipid extracts from cells was determined by HPLC following its derivatization with *o*-phthalaldehyde as described (13). The internal standard C17SPH (SPH with 17 carbons) was added to enzymatic reaction mixtures or lipid extracts from cells. The enzymatic reaction mixtures or lipid extracts were then treated for 30 min at 37 °C with 0.125 M methanolic KOH to hydrolyze phospholipids. After Bligh-Dye extraction (12), SPH in the enzymatic reactions or lipid extracts was derivatized with *o*-phthalaldehyde before HPLC analysis was performed. The content of SPH in each sample was normalized to the phospholipid level (P_i), which was determined as described (14).

Analysis of Enzymatic Kinetic Parameters—The hydrolysis of ceramides by ACER2 microsomes was described using the Michaelis-Menten equation, and the values of Michaelis-Menten constant (K_m) and maximum velocity (V_m) were estimated from individual experiments according to nonlinear regression using GraphPad Prism software (version 4.03). The results were expressed as mean ± S.D.

ESI/MS/MS Analysis for Sphingolipids—Sphingolipids were determined by electrospray ionization-mass spectrometric analysis (ESI/MS/MS) as described (15). Briefly, cells were harvested after being washed with ice-cold 25 mM Tris-HCl buffer (pH 7.4) containing 150 mM NaCl. Fifty μl of a mixture (1 μM) of internal sphingolipid standards including C17SPH, C17SPH-1-phosphate, D-e-C_{16}-ceramide (d17:1/16:0), and D-e-$_{18}$-ceramide (d17:1/18:0) was added to each cell pellet sample. Each cell sample was then extracted with 4 ml of the ethyl acetate/isopropyl alcohol/water (60/30/10%, v/v) solvent system. After centrifugation, 1 ml of lipid extracts was used for P_i determination, and the remaining for ESI/MS/MS. The lipid extracts were dried under a stream of nitrogen gas. For ESI/MS/MS, dried lipid extracts was dissolved in 100 μl of acidified (0.2% formic acid) methanol, and injected on the HP1100/TSQ 7000 LC/MS system and the gradient was eluted from the BDS Hypersil C8, 150 × 3.2 mm, 3-μm particle size column, with a 1.0 mM methanolic ammonium formate, 2 mM aqueous ammonium formate mobile phase system. Peaks corresponding to the target analytes and internal sphingolipid were collected and processed using Xcalibur software. Quantitative analyses of endogenous sphingolipids were based on calibration curves generated by spiking an artificial matrix with known amounts of the target analyte synthetic standards and an equal amount of the internal sphingolipid. The target analyte/internal sphingolipid peak area ratios were compared with the calibration curves using a linear regression model. Levels of the particular sphingolipids were normalized to phospholipids (P_i), and expressed as sphingolipids/P_i (pmol/μmol).

RESULTS

Effects of pH and Cations on in Vitro ACER2 Activity—To biochemically characterize ACER2, we first overexpressed ACER2 in yeast mutant cells (Δ*ypc1*Δ*ydc1*) in which both yeast alkaline ceramidase genes *YPC1* and *YDC1* were deleted (8–10). Unlike mammalian cells in which 5 ceramidases have been found, yeast cells only express the two alkaline ceramidases, YPC1p and YDC1p, according to the sequence of the yeast genome. Therefore, Δ*ypc1*Δ*ydc1* mutant cells lack any endogenous ceramidase activity due to the deletion of both the yeast alkaline ceramidases. This was confirmed by *in vitro* ceramidase activity assays using C_{12}-NBD-ceramide, a common synthetic substrate for most known ceramidases (data not shown). Therefore, Δ*ypc1*Δ*ydc1* cells overexpressing ACER2, which are termed Δypc1Δydc1ACER2 cells, should have ceramidase activity encoded solely by the recombinant ACER2. This yeast expression system allowed us to characterize recombinant ACER2 biochemically using microsomes isolated from Δypc1Δydc1ACER2 cells, ACER2 microsomes. Western blot analysis showed that ACER2 was expressed in Δ*ypc1*Δ*ydc1*ACER2 cells but not in control cells (Δ*ypc1*Δ*ydc1*YES2) that were transformed with the empty vector pYES2 only (Fig. 1*A*). *In vitro* activity assays demonstrated that ACER2 microsomes, but not YES2 microsomes from Δ*ypc1*Δ*ydc1*YES2 cells, exhibited high ceramidase activity at pH 8.0 toward D-e-$C_{24:1}$-ceramide (Fig. 1*B*), a previously identified substrate of ACER2 (6).

To determine the pH optimum of ACER2, we measured ceramidase activity in ACER2 microsomes at different pH values. ACER2 microsomes had the highest ceramidase activity on D-e-$C_{24:1}$-ceramide at pH 7.5 to 9.0 (Fig. 1*C*). In contrast, at a pH below 7 or above 9.5, ceramidase activity in ACER2 microsomes declined sharply, suggesting that ACER2 has a narrow alkaline pH optimum.

Because we previously showed that the ACER2 homologues ACER1 and ACER3/haPHC are activated by Ca^{2+} (8, 16), all earlier ACER2 *in vitro* activity assays were performed in the presence of 5 mM $CaCl_2$. To determine whether Ca^{2+} is indeed required for ACER2 activity, we measured activity of ACER2 microsomes using D-e-$C_{24:1}$-ceramide as substrate at pH 9.0 in the absence or presence of various concentrations of $CaCl_2$. ACER2 microsomes exhibited minor ceramidase activity in the absence of $CaCl_2$, but microsomal ceramidase activity was increased with an increasing concentration of $CaCl_2$ (Fig. 1*D*), suggesting that Ca^{2+} is important for *in vitro* ACER2 activity. To determine whether Ca^{2+} is a specific cation that activates ACER2, we tested the effects of other cations on ACER2 activity. Zn^{2+} or Cu^{2+} inhibited basal ceramidase activity in ACER2 microsomes, and Mg^{2+} or Mn^{2+} had no effect on ceramidase activity in ACER2 microsomes (Fig. 1*D*). These results suggest that Ca^{2+} specifically activates ACER2 *in vitro*.

ACER2 Enzyme Kinetics—To study the kinetics of ACER2, ceramidase activity in ACER2 microsomes was determined in the presence of various concentrations of D-e-$C_{24:1}$-ceramide, a

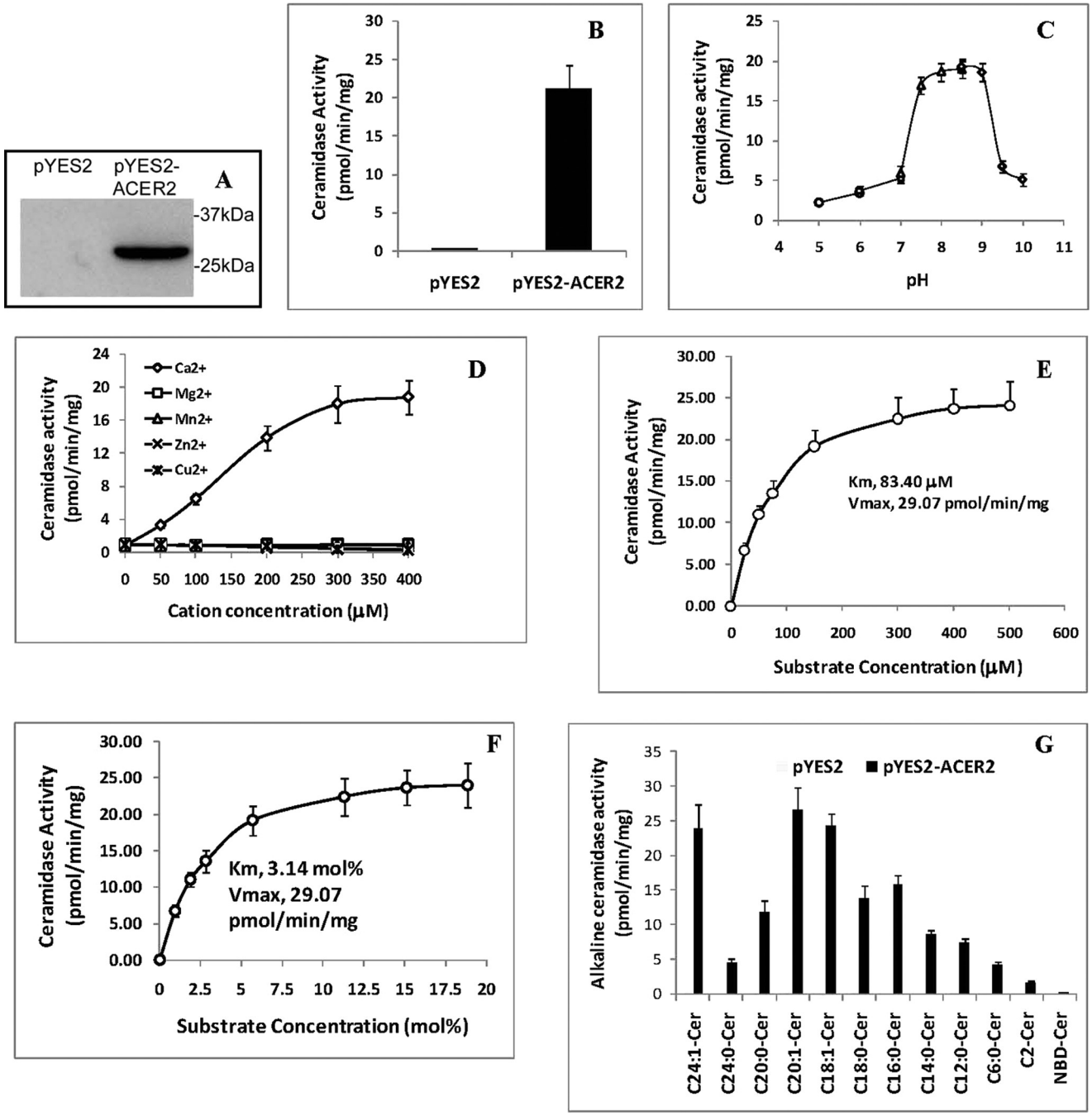

FIGURE 1. **Biochemical properties of ACER2.** *A*, microsomes were isolated from Δ*ypc1*Δ*ydc1*ACER2 and Δ*ypc1*Δ*ydc1*YES2 cells grown in galactose medium, and ACER2 expression was determined by Western blot analysis using the anti-FLAG antibody. Each lane contained microsomes equivalent to 20 μg of protein. *B*, microsomes (40 μg of protein per reaction) were measured for *in vitro* ceramidase activity using D-e-$C_{24:1}$-ceramide (150 μM) as substrate. Note that Δ*ypc1*Δ*ydc1*ACER2 (*pYES2-ACER2*) but not Δ*ypc1*Δ*ydc1*YES2 microsomes (*pYES2*) exhibited ceramidase activity. *C*, Δ*ypc1*Δ*ydc1*ACER2 and Δ*ypc1*Δ*ydc1*YES2 microsomes were measured for ceramidase activity on D-e-$C_{24:1}$-ceramide (150 μM) in different buffer systems with 0.15% (v/v) Triton X-100. *Circle*, *square*, *triangle*, and *diamond* represent 20 mM acetate, Pipes, Tris-HCl, and glycine-NaOH buffer, respectively. *D*, Δ*ypc1*Δ*ydc1*ACER2 microsomes were measured for ceramidase activity on D-e-$C_{24:1}$-ceramide (150 μM) at pH 9.0 in the presence of various cations at increasing concentrations. *E* and *F*, Δ*ypc1*Δ*ydc1*ACER2 microsomes were measured for ceramidase activity at pH 9.0 using different concentrations of D-*e*-$C_{24:1}$-ceramide as substrate in the presence of a fixed concentration (0.15%, v/v) of Triton X-100 and 1 mM $CaCl_2$. Alkaline ceramidase activity (*V*) was plotted as a function of the concentration ([S]) of D-e-$C_{24:1}$-ceramide, and the apparent K_m and V_{max} values for D-e-$C_{24:1}$-ceramide were determined using GraphPad Prism according to the nonlinear regression model. Substrate concentrations are expressed as either micormolar (*E*) or mol % (*F*). *G*, Δ*ypc1*Δ*ydc1*ACER2 or Δ*ypc1*Δ*ydc1*YES2 microsomes were measured for ceramidase activity at pH 9.0 with different ceramides as substrates at the same concentration (300 μM). Note that no activity was detected in the control microsomes when any substrate was used. Data represent the mean ± S.D. of three independent experiments.

major ceramide species found in mammalian cells. A plot of the reaction velocity (*V*) as a function of the substrate concentration (S) obeyed Michaelis-Menten kinetics (Fig. 1*E*). The apparent K_m and V_{max} values for D-e-$C_{24:1}$-ceramide were computed to be 81.40 ± 10.21 μM (3.14 mol %) and 27.07 ± 3.74 pmol/min/mg, respectively.

ACER2 Substrate Specificity—To determine the substrate specificity of ACER2, we measured ceramidase activity in

TABLE 1

K_m and V_{max} values of ACER2 for different substrates

Δ*ypc1*Δ*ydc1*ACER2 microsomes (40 μg of proteins per reaction) were measured for ceramidase activity at pH 9.0 using different concentrations of various ceramides as substrates in the presence of Triton X-100 (0.15%, v/v) and $CaCl_2$ (1 mM). The apparent K_m and V_{max} values were computed according to nonlinear regression by GraphPad Prism software. Data represent mean ± S.D. of three independent experiments.

Substrates	K_m	V_{max}	V_{max}/K_m
	μM/mol %	pmol/min/mg	μM
$C_{6:0}$-Cer	224.16 ± 37.51/8.45 ± 1.41	5.04 ± 0.72	0.02 ± 0.00
$C_{12:0}$-Cer	133.83 ± 17.88/5.05 ± 0.67	10.67 ± 1.54	0.08 ± 0.02
$C_{14:0}$-Cer	114.61 ± 13.28/4.32 ± 0.50	11.37 ± 1.41	0.10 ± 0.03
$C_{16:0}$-Cer	98.52 ± 11.79/3.71 ± 0.44	23.70 ± 3.18	0.24 ± 0.03
$C_{18:0}$-Cer	94.81 ± 10.06/3.57 ± 0.38	26.11 ± 3.47	0.28 ± 0.05
$C_{18:1}$-Cer	77.31 ± 8.43/2.91 ± 0.32	35.42 ± 5.10	0.46 ± 0.07
$C_{20:0}$-Cer	91.47 ± 9.79/3.45 ± 0.37	28.94 ± 3.61	0.32 ± 0.04
$C_{20:1}$-Cer	72.11 ± 8.52/2.71 ± 0.32	38.16 ± 4.74	0.53 ± 0.08
$C_{24:0}$-Cer	143.2 ± 18.16/5.39 ± 0.68	6.74 ± 0.87	0.05 ± 0.00
$C_{24:1}$-Cer	81.40 ± 10.21/3.06 ± 0.38	27.07 ± 3.78	0.33 ± 0.06

ACER2 microsomes using various ceramide species at 300 μM as substrates. As shown in Fig. 1*F*, ACER2 microsomes had high activity toward D-*e*-$C_{24:1}$, $C_{20:0}$, $C_{20:1}$, $C_{20:4}$, $C_{18:0}$, $C_{18:1}$, or $C_{16:0}$-ceramide, moderate activity toward D-e-$C_{24:0}$, $C_{14:0}$, $C_{12:0}$, or $C_{6:0}$-ceramide, and minor activity toward D-*e*-$C_{2:0}$-ceramide. To identify the best substrate(s) of ACER2, we determined the apparent K_m and V_{max} values of ACER2 for all the above ceramide species except for $C_{2:0}$-ceramide. As listed in Table 1, the V_{max}/K_m ratios were decreased in the following order: unsaturated long-chain ceramides ($C_{18:1}$, $C_{20:1}$, or $C_{20:4}$-ceramide) > saturated long-chain ceramides (D-e-$C_{16:0}$, $C_{18:0}$, or $C_{20:0}$-ceramide) > unsaturated very long-chain ceramide (D-e-$C_{24:1}$-ceramide) > saturated medium-chain ceramides (D-e-$C_{12:0}$ and $C_{14:0}$-ceramides) > saturated very long-chain ceramide (D-e-$C_{24:0}$) > short chain ceramide (D-e-$C_{6:0}$). These results suggest that unsaturated long-chain ceramides are the best substrates for ACER2, and saturated long-chain ceramides and unsaturated very long-chain ceramides are good substrates of ACER2, whereas saturated very long-chain ceramides and short-chain ceramides were poor substrates of ACER2.

Effect of Ca^{2+} on ACER2 Cellular Activity—We demonstrated that *in vitro* ACER2 activity was significantly increased by Ca^{2+} in the micromolar concentration range. Because ACER2 is a transmembrane Golgi enzyme, its cellular activity may require Ca^{2+} in the cytosol or the lumen of the Golgi complex. To test this possibility, we determined whether depletion of intracellular Ca^{2+} inhibited ACER2 activity in cells. We measured ACER2 cellular activity according to its ability to generate SPH in cells. We previously generated an ACER2 overexpressing cell line, ACER2-TET-ON cells in which ACER2 overexpression is under the control of a tetracycline (TET)-induced promoter system, CMV-TET-ON (6). In ACER2-TET-ON cells, ACER2 overexpression was induced in the presence of TET but not ethanol (Et), the vehicle control (Fig. 2*A*). ACER2-TET-ON cells grown in the presence of Et or TET were incubated in Ca^{2+}-free medium (SMEM) and treated with 50 μM BAPTA-AM, a cell permeable Ca^{2+}-chelator that depletes free cytosolic Ca^{2+}. Confocal microscopy demonstrated that treatment with BAPTA-AM at this concentration completely depleted free cytosolic Ca^{2+}, as indicated by a lack of fluorescence in the cytoplasm in cells loaded with a cell-permeable Ca^{2+} indicator FLUO-4 AM (Fig. 2*B*). HPLC showed that treatment with BAPTA-AM only slightly inhibited the TET-induced generation of SPH in ACER2-TET-ON cells (Fig. 2*C*), suggesting that free cytosolic Ca^{2+} is not required for cellular ACER2 activity. We then determined whether a reduction of the content of Ca^{2+} in the lumen of the Golgi complex ($[Ca^{2+}]_g$) had any effect on ACER2 activity in cells. To date, although the pharmacological agents that deplete Ca^{2+} specifically from the lumen of the Golgi complex are unavailable, it has been shown that treatment of HeLa cells with a relatively high concentration (≥2 μM) of thapsigargin (THAP), an inhibitor of sarcoplasmic/ER Ca^{2+}-ATPases, significantly decreases $[Ca^{2+}]_g$ (17, 18). Therefore, ACER2-TET-ON cells grown in the presence of Et or TET were treated with 2 μM THAP or DMSO, the vehicle control. HPLC demonstrated that treatment with THAP markedly inhibited the TET-induced generation of SPH in ACER2-TET-ON cells (Fig. 2*C*), suggesting that decreasing $[Ca^{2+}]_g$ and $[Ca^{2+}]$ in other intracellular Ca^{2+} stores inhibits cellular ACER2 activity.

Because THAP reduces not only $[Ca^{2+}]_g$ but also $[Ca^{2+}]$ in the lumen of the endoplasmic reticulum (ER) ($[Ca^{2+}]_{ER}$), which has been shown to affect the trafficking of some proteins from the ER to the other organelles, treatment with THAP may affect the cellular localization of ACER2. To exclude this possibility, we determined whether treatment with THAP affected the localization of ACER2 to the Golgi complex. ACER2-TET-ON cells grown in the presence of TET were treated with THAP or DMSO before cells were fixed and stained with anti-ACER2 antibody. Confocal microscopy demonstrated that both the anti-ACER2 antibody staining patterns and intensities were similar in ACER2-TET-ON cells treated with THAP and DMSO, respectively (Fig. 2*D*), suggesting that THAP alters neither the cellular localization of ACER2 nor its expression.

Because ceramides, the substrates of ACER2, are synthesized in the ER, decreasing $[Ca^{2+}]_{ER}$ may deplete the cellular substrates of ACER2 by inhibiting ceramide biosynthesis. ACER2-TET-ON cells grown in the presence of Et or TET were treated with THAP or DMSO for 2 h before ceramides were analyzed. ESI/MS/MS demonstrated that compared with treatment with DMSO, treatment with THAP increased rather than decreased ceramides in ACER2-TET-ON cells grown in the presence of either Et or TET (Fig. 2*E*), suggesting that decreasing $[Ca^{2+}]_{ER}$ and other intracellular stored Ca^{2+} does not inhibit the biosynthesis of ceramides in cells. Consistent with the inhibitory effect of THAP on cellular ACER2 activity, treatment with THAP inhibited the ACER2 overexpression-induced decrease in cellular ceramides (Fig. 2*E*), further supporting that depletion of intracellular stored Ca^{2+} inhibits cellular ACER2 activity.

Because ceramides are transported from the ER to the Golgi complex, depletion of intracellular stored Ca^{2+} may block the trafficking of ceramides to the Golgi complex. To exclude this possibility, we determined whether depletion of intracellular Ca^{2+} inhibits sphingomyelin biosynthesis, which requires ceramides in the Golgi complex. ESI/MS/MS demonstrated that compared with treatment with DMSO, treatment with THAP increased rather than decreased the levels of sphingomyelins in ACER2-TET-ON cells grown in the presence of Et or TET (Fig. 2*F*), suggesting that depletion of luminal Ca^{2+} does not affect

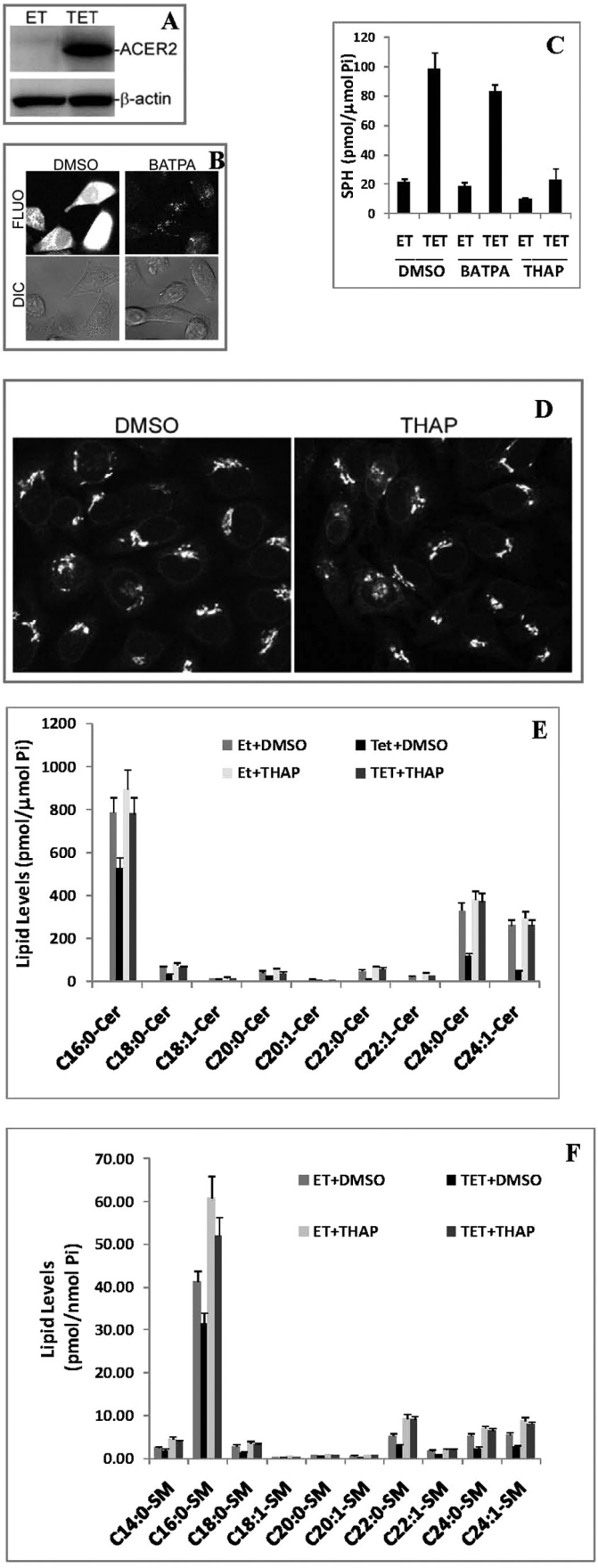

the trafficking of ceramides to the Golgi complex. Consistent to their inhibitory effect on ACER2 cellular activity, treatment with THAP inhibited the ACER2 overexpression-induced decrease in the levels of sphingomyelins in ACER2-TET-ON cells (Fig. 2*F*).

Taken together, these aforementioned results suggest that THAP inhibits ACER2 cellular activity likely by depleting Ca^{2+} from the lumen of the Golgi complex not by depleting its substrates. Golgi Ca^{2+}, therefore, is required for ACER2 cellular activity.

Amino and Carboxyl Termini of ACER2 Are Oriented in Golgi Lumen and Cytosol, Respectively—ACER2 is a Golgi protein that was predicted by the pSORTII program to have 7 putative TMDs (Fig. 3*A*). However, its membrane topology remains unclear. To this end, we determined the orientation of its N and C termini. Because the FLAG epitope tag is attached to the N terminus of the recombinant ACER2 (FLAG-ACER2) expressed in ACER2-TET-ON cells, the N terminus of FLAG-ACER2 can be recognized by an anti-FLAG antibody. The C terminus of FLAG-ACER2 can be recognized by the anti-ACER2 antibody that was raised from a peptide immunogen corresponding to the C terminus of ACER2 (Fig. 3*A*). ACER2-TET-ON cells grown in the presence of TET were fixed and permeablized with digitonin or Triton X-100, respectively. Treatment with a low concentration (<5 μg/ml) of digitonin at 4 °C has been shown to selectively permeabilize the plasmas membrane but not intracellular membrane systems, such as the Golgi complex (11), whereas treatment with Triton X-100 permeabilizes both the plasmas membrane and the Golgi complex. The differentially permeabilized ACER2-TET-ON cells were immunostained with the anti-FLAG monoclonal and anti-ACER2 polyclonal antibody simultaneously. FLAG-ACER2 was stained with the anti-ACER2 antibody but not with the anti-FLAG antibody in digitonin-treated ACER2-TET-ON cells, whereas it was stained with both antibodies in Triton X-100-treated cells (Fig. 3*B*).

FIGURE 2. **Cellular ACER2 activity is inhibited by depletion of Ca^{2+} from Golgi lumen.** *A*, ACER2-TET-ON cells were grown in the presence of Et or TET (10 ng/ml) for 48 h before Western blot analysis was performed using the anti-ACER2 antibody. For normalization of equal loading, the membrane blot was stripped of the anti-ACER2 antibody, and reprobed with anti-β-actin antibody. *B*, ACER2-TET-ON cells were loaded with Fluo-4 AM (4 μM; Invitrogen) according to the manufacturer's instructions. After being washed 3 times with Ca^{2+}-free medium SMEM, ACER2-TET-ON cells loaded with Fluo-4 AM were treated with 50 μM BAPTA-AM (*BAPTA*) or DMSO, the vehicle control, for 1 h before being imaged on the LSM Meta 510 confocal microscope. Note that BAPTA-AM treatment markedly reduced the fluorescent intensity of Fluo-4 AM in the cytoplasm of ACER2-TET-ON cells. *C*, ACER2-TET-ON cells grown in the presence of Et or TET were treated for 1 h with 50 μM BAPTA-AM, 2 μM THAP (*THAP*), or DMSO before the levels of SPH were determined by HPLC. *D*, ACER2-TET-ON cells grown in the presence of TET were treated for 2 h with 2 μM THAP or DMSO before being fixed with 3.75% paraformaldehyde in PBS for 10 min. The fixed cells were immunostained with the anti-ACER2 antibody followed by anti-rabbit IgG antibody-rhodamine conjugate before being imaged on the confocal microscope. Note that THAP treatment did not alter the cellular localization of ACER2 in ACER2-TET-ON cells. *E* and *F*, ACER2-TET-ON cells were grown in the presence of Et or tetracycline (*TET*) (10 ng/ml) for 48 h before they were treated for 2 h with 2 μM THAP or DMSO. The cells were harvested and subjected to ESI/MS/MS analysis for the levels of ceramides (*C*), sphingoid bases and their phosphates (*D*), and sphingomyelins (*E*). Data represent the mean ± S.D. of three independent experiments performed in duplicate.

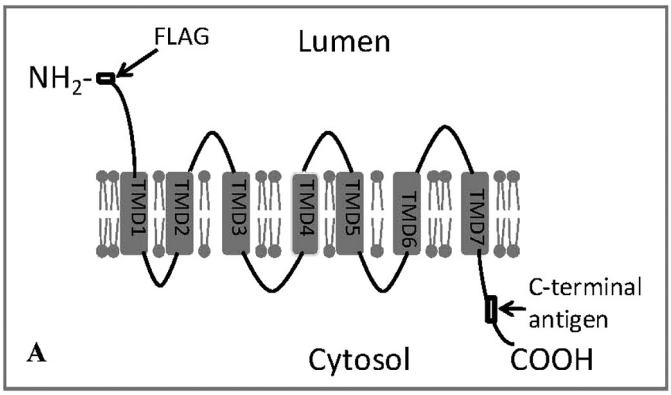

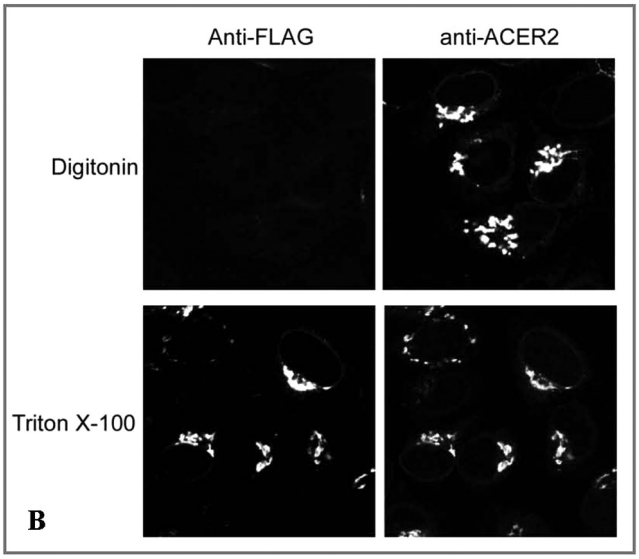

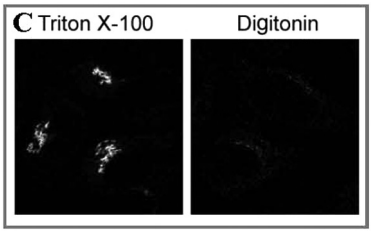

FIGURE 3. **Amino and carboxyl termini of the ACER2 face of Golgi lumen and cytosol, respectively.** *A*, the predicted membrane topology of ACER2 according to the pSORTII program. *B*, ACER2-TET-ON cells grown in the presence of TET (10 ng/ml) were fixed with paraformaldehyde. The fixed cells were permeabilized for 10 min at 4 °C with 3 μg/ml of digitonin or 0.05% Triton X-100. The cells were then blocked with BSA before being incubated for 1 h with the anti-FLAG antibody and anti-ACER2 antibody. After washing with PBS, the cells were incubated for 1 h with the anti-rabbit IgG antibody-rhodamine and anti-mouse IgG antibody-FITC. After a final wash with PBS, the cells were imaged on a confocal microscope (Zeiss LSM510 Meta). Note that the N terminus labeled with the anti-FLAG antibody/anti-mouse IgG antibody-FITC was in the lumen of the Golgi complex, whereas the C terminus labeled with the anti-ACER2 antibody/anti-rabbit IgG antibody-rhodamine faced the cytosol. *C*, ACER2-TTE-ON cells grown in the presence of TET (10 ng/ml) were fixed and permeabilized with Triton X-100 or digitonin as described in *B* before being immunostained with anti-mannosidase II antibody, which recognizes a luminal domain of the Golgi mannosidase II. Note that mannosidase II was labeled by its antibody in Triton X-100-permeabilized but not in digitonin-permeabilized cells. Image data represent one of several experiments with similar results.

It should be noted that the plasmas membrane was indeed permeabilized in digitonin-treated cells because anti-ACER2 antibody entered the cells to bind FLAG-ACER2. This suggests that like anti-ACER2 antibody, anti-FLAG antibody also reached the cytosol in digitonin-treated cells and that it failed to stain ACER2 due to a failure to reach the lumen of the Golgi complex. To confirm that the Golgi complex is indeed permeabilized by Triton X-100 but not digitonin, we performed immunostaining with an antibody that recognizes a luminal domain of mannosidase II, another Golgi protein. It was found that mannosidase II was stained with its antibody in Triton X-100-treated ACER2-TET-ON cells but not in digitonin-treated cells, confirming that the plasma membrane but not the Golgi complex was permeabilized in digitonin-treated cells, whereas both the plasmas membrane and the Golgi complex were permeabilized in Triton X-100-treated cells (Fig. 3*C*). These results suggest that the N terminus of ACER2 is oriented in the lumen of the Golgi complex, and its C terminus in the cytosol.

Luminal ACER2 N-terminal Tail Is Important for ACER2 Activity—According to protein sequence alignment, we previously showed that all known alkaline ceramidases have a conserved region adjacent to the first putative TMD (6), suggesting that the N-terminal tail may be important for ACER2 activity. To address this possibility, we determined whether deletion of the N-terminal tail affected ACER2 activity. We generated an expression construct, pcDNA3-ACER2ΔN36, that directs the expression of an ACER2 mutant, ACER2ΔN36, that lacks the N-terminal tail (the first 36 amino acid residues) (Fig. 4*A*). pcDNA3-ACER2ΔN36, pcDNA3-ACER2 (the expression construct for wild-type ACER2), or empty vector pcDNA3-FLAG were transiently transfected into HeLa cells. To facilitate its expression detection, the FLAG epitope tag was attached to the N termini of both ACER2 and ACER2ΔN36. Western blot analysis with anti-FLAG antibody detected a protein band in HeLa cells transfected with pcDNA3-ACER2ΔN36 or pcDNA3-ACER2, but not in HeLa cells transfected with pcDNA3 (Fig. 4*B*). As expected, the protein band in HeLa cells transfected with pcDNA3-ACER2 is greater in apparent molecular mass than the major protein band in HeLa cells transfected with pcDNA3-ACER2ΔN36.

To determine the effect of the depletion of the N terminus on ACER2 activity, we measured alkaline ceramidase activity in the microsomes isolated from HeLa cells overexpressing ACER2ΔN36 or ACER2 or from cells transfected with the empty vector. The results showed that, compared with the control empty vector, overexpression of ACER2 but not ACER2ΔN36 increased alkaline ceramidase activity toward D-e-C_{16}-ceramide (Fig. 4*C*), suggesting that depletion of the N-terminal tail inhibits ACER2 activity. To further confirm this concept, we determined whether ACER2ΔN36 overexpression also failed to increase the generation of SPH in cells. HPLC analysis demonstrated that compared with transfection with the empty vector, HeLa cells transfected with pcDNA3-ACER2 but not pcDNA3-ACER2ΔN36 had increased levels of SPH in HeLa cells (Fig. 4*D*), confirming that the N-terminal tail is important for ACER2 activity.

Because there is a possibility that ACER2ΔN36 has residue activity that may be too low to be detected in cells with endogenous ACER2 activity, we overexpressed ACER2ΔN36 in Δypc1Δydc1 yeast cells that lack any endogenous alkaline cer-

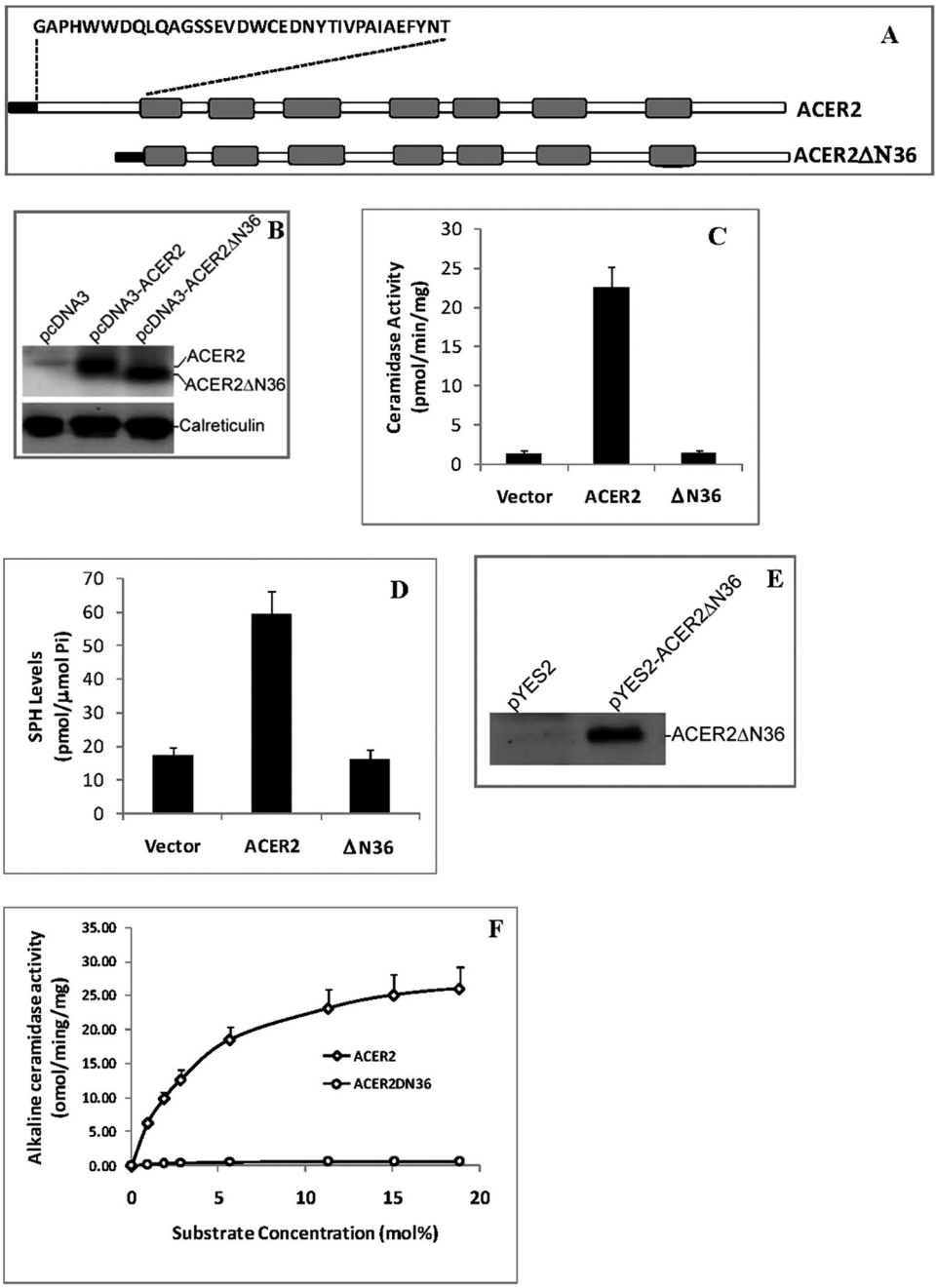

FIGURE 4. **The N-terminal tail is essential for ACER2 activity.** *A*, the structures of wild-type ACER2 (ACER2) and its mutant ACER2ΔN36 lacking the first 36 amino acid residues. The *gray bars* represent the putative TMs, *open bars* the N- and C-terminal tails and luminal and cytosolic loops, and the *black bar* the FLAG epitope tag. The sequence of the N-terminal tail of ACER2 is shown. *B*, HeLa cells were transfected for 48 h with pcDNA3, pcDNA3-ACER2, or pcDNA3-ACER2ΔN36 before Western blot analysis was performed with the anti-FLAG antibody. For normalization of equal loading, the membrane blot was reprobed with the anti-calreticulin antibody after being stripped of the anti-FLAG antibody. *C*, microsomes were isolated from HeLa cells as described in *B*, and microsomal alkaline ceramidase activity was determined on D-e-C_{16}-ceramide as substrate. *D*, SPH levels were determined by HPLC in HeLa cells as described in *B*. *E*, microsomes were isolated from Δ*ypc1*Δ*ydc1*ACER2ΔN36 and Δ*ypc1*Δ*ydc1*YES2 cells grown in galactose medium, and ACER2ΔN36 expression was analyzed by Western blot using the anti-FLAG antibody. Each lane contained microsomes equivalent to 20 μg of protein. *F*, microsomes (40 μg of protein per reaction) from Δ*ypc1*Δ*ydc1*ACER2ΔN36 or Δ*ypc1*Δ*ydc1*ACER2 were measured for *in vitro* ceramidase activity on various concentrations of D-e-C_{16}-ceramide. Data represent the mean ± S.D. of three independent experiments performed in duplicate.

amidase activity, and determined ACER2ΔN36 kinetics. We generated a yeast strain, Δypc1Δydc1ACER2ΔN36, that overexpresses ACER2ΔN36 under control of the Gal1 promoter as described under "Experimental Procedures." Western blot analysis showed that the expression of ACER3Δ36 was detected in Δypc1Δydc1ACER2ΔN36 cells grown in galactose-containing medium but not in control Δypc1Δydc1YES2 cells (Fig. 4*E*). Microsomes (termed ACER2ΔN36 microsomes) were isolated from Δypc1Δydc1ACER2ΔN36 grown in the galactose medium, and alkaline ceramidase activity was determined using D-e-C_{16}-ceramide as substrate at various concentrations. ACER2 microsomes were also included in this study as a positive control. As shown in Fig. 4*F*, alkaline ceramidase activity in ACER2 microsomes was increased with increasing concentrations of D-e-C_{16}, whereas alkaline ceramidase activity was not detected in ACER2ΔN36 microsomes at any concentration of D-e-C_{16}-ceramide, suggesting that ACER2ΔN36 indeed lacks detectable alkaline ceramidase activity. Taken together, the aforementioned results suggest that the N terminus of ACER2 is required for ACER2 activity.

The Very End of the N Terminus of ACER2 Is Not Required for Its Activity—To elucidate the region in the N-terminal tail essential for ACER2 activity, we determined whether deleting the first 13 amino acid residues that are not conserved to the other alkaline ceramidases affected ACER2 activity. Using the same strategy for the generation of pcDNA3-ACER2ΔN36, we generated the expression construct pcDNA3-ACER2ΔN13 that directs the expression of ACER2ΔN13, an ACER2 mutant with deletion of the first 13 amino acid residues (Fig. 5*A*). HeLa cells were transfected with pcDNA3, pcDNA3-ACER2, and pcDNA3-ACER2ΔN13, respectively. Western blot analysis demonstrated that ACER2ΔN13 was expressed in HeLa cells transfected with pcDNA3-ACER2ΔN13 but not in cells transfected with pcDNA3 (Fig. 5*B*). Because there is only a small difference in molecular mass between ACER2 and ACER2ΔN13, they were very similar in electrophoretic mobility. Microsomes isolated from HeLa cells transfected with pcDNA3-ACER2ΔN13 had higher alkaline ceramidase activity

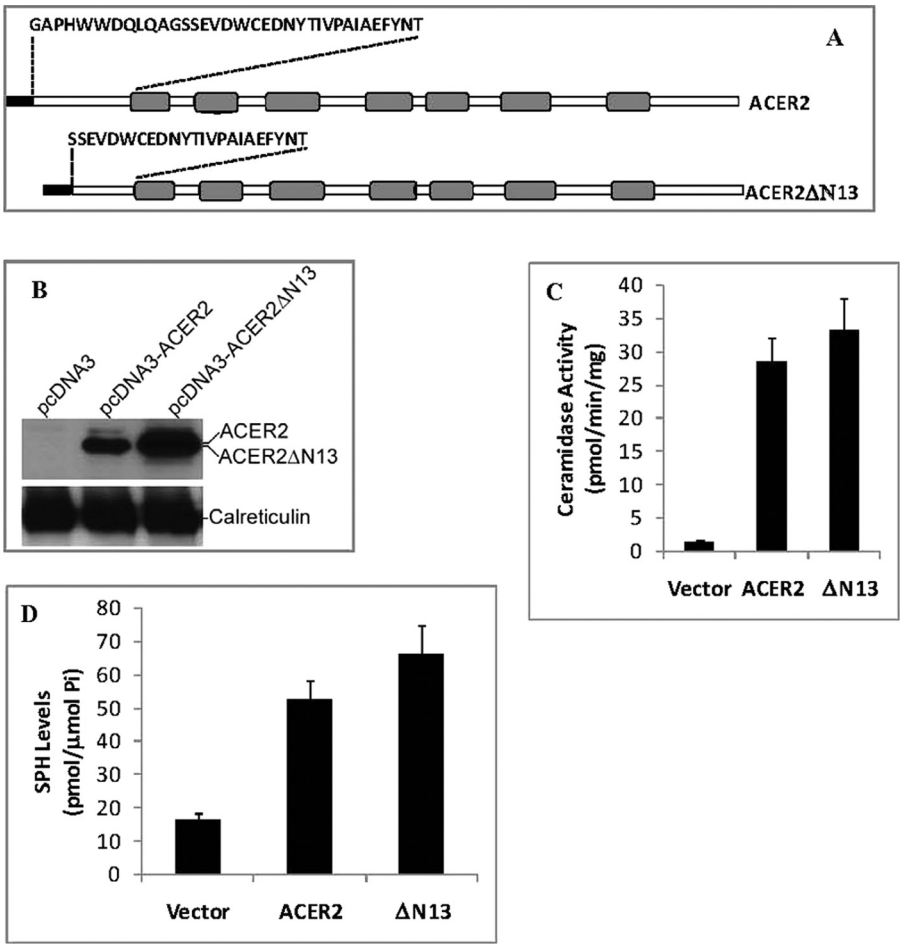

FIGURE 5. **The first 13 amino acid residues in the N-terminal tail are not required for ACER2 activity.** *A*, the structures of wild-type ACER2 (ACER2) and its mutant ACER2ΔN13 lacking the first 13 amino acid residues. The *gray bars* represent the putative TMs, *open bars* the N- and C-terminal tails and luminal and cytosolic loops, and the *black bar* the FLAG epitope tag. The sequences of the N-terminal tails of ACER2 and ACER2ΔN13 are shown. *B*, HeLa cells were transfected for 48 h with pcDNA3, pcDNA3-ACER2, or pcDNA3-ACER2ΔN13 before Western blot analysis was performed. *C*, microsomes were isolated from HeLa cells transfected with the indicated plasmids as described in *B*, and microsomal alkaline ceramidase activity was determined on D-e-C_{16}-ceramide as substrate. *D*, SPH levels were determined by HPLC in HeLa cells transfected with the indicated plasmids as described in *B*. Data represent the mean ± S.D. of three independent experiments.

than microsomes isolated from HeLa cells transfected with the empty vector pcDNA3 (Fig. 5*C*), suggesting that the first 13 amino acids are not required for ACER2 activity. To further confirm this concept, we determined whether overexpression of ACER2ΔN13 had any effect on the cellular levels of SPH. HPLC analysis demonstrated that similar to HeLa cells transfected with pcDNA3-ACER2, HeLa cells transfected with pcDNA3-ACER2ΔN13 had increased levels of SPH compared with HeLa cells transfected with the empty vector pcDNA3-FLAG (Fig. 5*D*), suggesting that ACER2ΔN13 retains ceramidase activity in cells. Taken together, the results shown in Figs. 4 and 5 indicate that the region between the 13th and 36th amino acid residues is necessary for ACER2 activity.

N Terminus Is Required for the Localization of ACER2 to the Golgi Complex—To determine whether deletion of the N terminus affected the cellular localization of ACER2, we compared the immunocytochemical staining pattern of ACER2ΔN13 or ACER2ΔN36 to that of ACER2. Cells transfected with pcDNA3-ACER2, ACER2ΔN13, or ACER2ΔN36 were immunostained with the monoclonal anti-FLAG antibody and the polyclonal antibody against giantin, a Golgi resident protein. Confocal microscopy demonstrated that the immunostaining pattern with the anti-FLAG antibody in cells expressing ACER2 but not ACER2ΔN13 or ACER2ΔN36 was the same as that with the anti-giantin antibody (Fig. 6*A*), suggesting that ACER2 but not its mutants is localized to the Golgi complex. Because both ACER2ΔN13 and ACER2ΔN36 exhibited an immunostaining pattern of the reticulum network, we predicted that both ACER2 mutants may be localized to the ER. To test this idea, HeLa cells expressing ACER2ΔN13 or ACER2ΔN36 were co-immunostained with the anti-FLAG antibody and an antibody against calreticulin, an ER resident protein. Confocal microscopy showed that the immunostaining pattern with the anti-FLAG antibody in HeLa cells expressing either ACER2ΔN13 or ACER2ΔN36 was similar but not identical to that with the anti-calreticulin antibody, whereas the immunostaining patterns with the anti-FLAG and anti-calreticulin antibodies, respectively, were different in HeLa cells expressing ACER2 (Fig. 6*B*), suggesting that both ACER2ΔN13 and ACER2ΔN36 are mainly localized to the ER. These results indicate that the region of the first 13 amino acids is essential for ACER2 to be localized to the Golgi complex.

Mistargeting of ACER2 Abolishes Its Role in Sphingosine-induced Inhibition of Protein Glycosylation without Affecting S1P Signaling—Our previous studies demonstrated that ACER2 overexpression activates the S1P/S1PR1 pathway by increasing the extracellular levels of S1P (6) while inhibiting protein glycosylation in the Golgi complex by increasing the levels of SPH in the Golgi complex (19). Because correct cellular localization is important for the biological function of the protein, we determined whether mistargeting of ACER2 to the ER affected its roles in cellular actions. First, we determined whether overexpression of ACER2ΔN13 increased the secretion of S1P to medium. To further exclude the role of ACER3ΔN36 in regulating S1P, we also determined whether its overexpression affected S1P release. HeLa cells were transiently transfected with pcDNA3-ACER2Δ13, pcDNA3ΔN36, pcDNA3-ACER2 (as a positive control), or pcDNA3 (as a negative control). At 24 h post-transfection, cells were washed several times with serum-free medium containing 0.1% BSA to remove any residue S1P left from serum. The cells were then incubated with

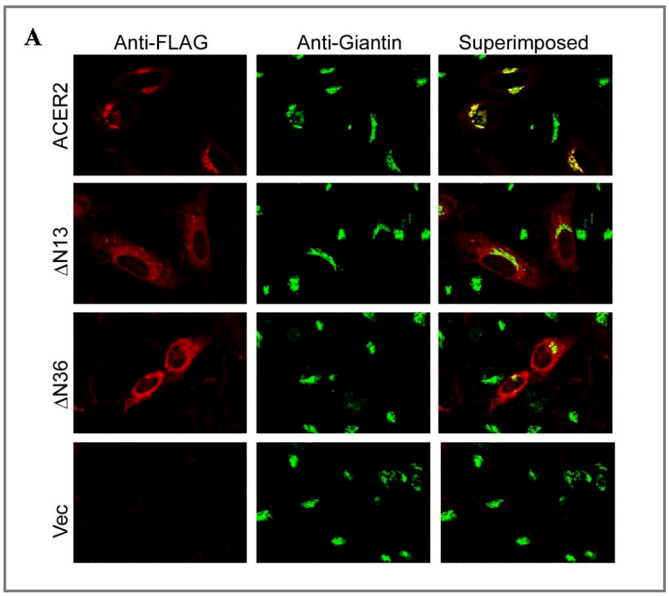

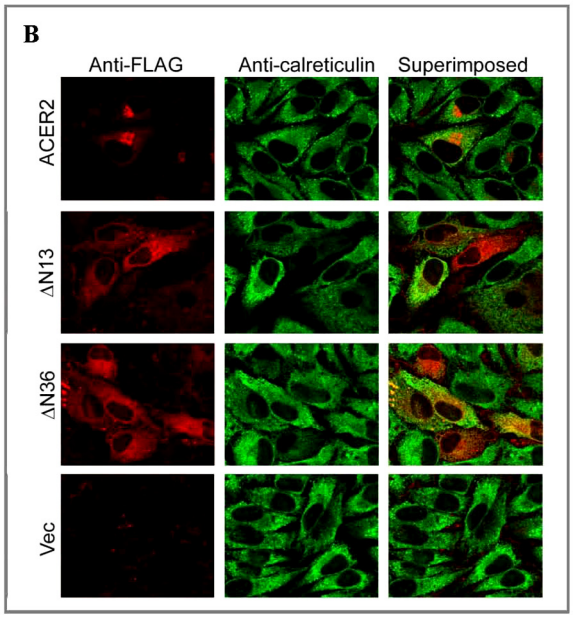

FIGURE 6. **Luminal N-terminal tail is essential for ACER2 localization to the Golgi complex.** *A*, HeLa cells transfected with pcDNA3-ACER2, pcDNA3-ACER2ΔN13, and pcDNA3-ACER2ΔN36 were co-stained with the monoclonal anti-FLAG and polyclonal anti-giantin antibodies, followed by the anti-mouse IgG antibody-rhodamine and anti-rabbit IgG antibody-FITC. Immunostained cells were imaged on the confocal microscope as described in the legend to Fig. 4*B*. *B*, HeLa cells transfected as described in *A* were co-stained with the monoclonal anti-FLAG and polyclonal anti-calreticulin antibodies, followed by the anti-mouse IgG antibody-rhodamine and anti-rabbit IgG antibody-FITC. Immunostained cells were imaged on the confocal microscopy. Note that cells transfected with the vector pcDNA3 exhibited very low background staining with the anti-FLAG antibody.

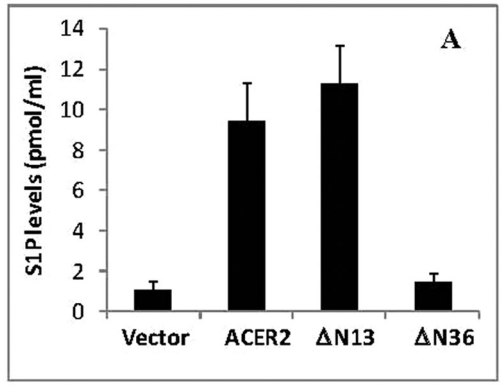

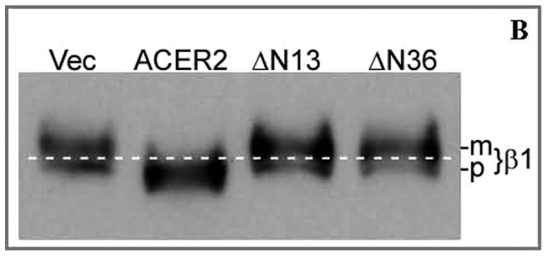

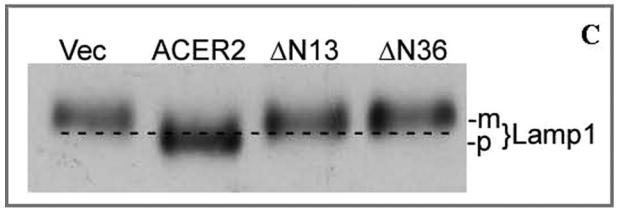

FIGURE 7. **ACER2 Golgi localization is required for its ability to regulate protein glycosylation but not for its ability to regulate S1P secretion.** *A*, HeLa cells grown in regular MEM were transfected with pcDNA3 (*Vector*), pcDNA3-ACER2 (*ACER2*), pcDNA3-ACER2ΔN13 (Δ*N13*), or pcDNA3-ACER2ΔN36 (Δ*N36*) for 24 h before being switched to serum-free MEM containing 0.1% BSA and a mixture of growth factors, including epidermal growth factor (20 ng/ml), fibroblast growth factor-1 (10 ng/ml), and insulin-like growth factor-1 (20 ng/ml). Conditioned medium was then collected and centrifuged at 3,000 × *g* to remove floating cells or cell debris. Total lipids in centrifuged conditioned medium were then extracted by the Bligh-Dyer method (12), and S1P levels were determined by ESI/MS/MS. Data represent the mean ± S.D. of three independent experiments. *B* and *C*, HeLa cells were transfected with pDNA3 (*Vec*), pcDNA3-ACER2, pcDNA3-ACER2ΔN13, and pcDNA3-ACER2ΔN36 for 48 h before Western blot analysis was performed with the anti-integrin β1 subunit (β1) antibody (*B*) or anti-Lamp 1 antibody (*C*). *m*, the β1 or Lamp1 mature form that is fully glycosylated in the Golgi complex; and *p*, the integrin β1 subunit or Lamp1 precursor that is partially glycosylated in the ER. Images are representative of two experiments with similar results.

serum-free medium containing 0.1% BSA and a mixture of growth factors, including epidermal growth factor (20 ng/ml), fibroblast growth factor-1 (10 ng/ml), and insulin-like growth factor-1 (20 ng/ml), which prevented cell death without introducing exogenous S1P. Twenty-four h later, the conditioned medium was collected and centrifuged to remove any cell debris. S1P was then extracted from the medium and quantified by ESI/MS/MS. The results demonstrated that cells overexpressing ACER2 or ACER2ΔN13, but not ACER2ΔN36 increased the levels of S1P secreted to medium compared with cells transfected with the empty vector (Fig. 7*A*), suggesting that ACER2ΔN13 mistargeting does not eliminate its ability to regulate the secretion of S1P, whereas ACER2ΔN36 lacks this ability.

Second, we determined whether the mistargeting of ACER2 affected its ability to inhibit the glycosylation of the β1 integrin subunit (β1). Western blot analysis demonstrated that overexpression of ACER2 but not ACER2ΔN13 or ACER2ΔN36 decreased the content of the fully glycosylated form of β1, the mature β1, while increasing that of the partially glycosylated form of β1, immature β1, or β1 precursor (Fig. 7*B*), suggesting that the mistargeting of ACER2 to the ER abolishes its ability to

inhibit protein glycosylation in the Golgi complex. As expected, the catalytically inactive ACER2ΔN36 mutant had no effect on β1 glycosylation (Fig. 7*B*).

To determine whether ACER2 overexpression has a general inhibitory effect on protein glycosylation in the Golgi complex, we investigated whether overexpression of ACER2 or ACER2ΔN13 has any effect on the glycosylation of Lamp1, a lysosome membrane-bound protein that is also highly glycosylated. Western blot analysis demonstrated that overexpression of ACER2 but not the mutants caused a shift in the electrophoretic mobility of Lamp1 (Fig. 7*C*), suggesting that expression of ACER2 but not ACER2ΔN13 or ACER2ΔN36 inhibits the glycosylation of Lamp1. These results suggest that Golgi ACER2 has a general inhibitory effect on protein glycosylation and that mistargeted ACER2 mutants lose this ability.

DISCUSSION

In this study, we took advantage of our previously generated yeast mutant strain that lacks any endogenous ceramidase activity to express a recombinant ACER2 and characterize it biochemically. We demonstrated that similar to its yeast and mammalian homologues, the recombinant ACER2 has an alkaline pH optimum for its *in vitro* activity. ACER2 has broad substrate specificity, catalyzing the hydrolysis of most mammalian ceramide species. *In vitro*, ACER2 is activated by the specific cation Ca^{2+}, and ACER2 requires Ca^{2+} in the lumen of the Golgi complex for its cellular activity. Our study for the first time revealed that luminal Ca^{2+} is required for the catabolism of sphingolipids. We also determined that the N-terminal tail is oriented in the lumen of the Golgi complex and is required for both ACER2 activity and Golgi localization. We also present evidence that Golgi localization is essential for ACER2 to regulate protein glycosylation. These studies provide a molecular and cellular basis for understanding the physiological and pathological function of ACER2.

We showed that ACER2 has broad substrate specificity, catalyzing the hydrolysis of various mammalian ceramide species with a preference for unsaturated long-chain ceramides. Consistent with its *in vitro* substrate specificity, we previously demonstrated that ACER2 catalyzes the hydrolysis of most ceramide species in cells because overexpression of ACER2 decreases their levels in HeLa cells (6). The role of ACER2 in catalyzing the hydrolysis of various ceramides in cells is further confirmed in this study. We previously demonstrated that ACER1, a homologue of ACER2, prefers ceramides with very long-chain unsaturated fatty acids with a minor activity toward ceramides with very long-chain saturated ceramides but had no activity toward saturated long-chain ceramides such as D-e-$C_{16:0}$-ceramide (16). Consistent with its substrate specificity, ACER1 only catalyzes the hydrolysis of very long-chain ceramides in cells as ACER1 overexpression causes a decrease in very long-chain ceramides (D-e-$C_{24:0}$-ceramide and D-e-$C_{24:1}$) but not long-chain ceramide (D-e-C_{16}-ceramide) or medium-chain ceramide (D-e-C_{14}-ceramide) (16). Very recently, we demonstrated that ACER3, another ACER2 homologue that was previously referred to as haPHC (8), only used unsaturated long-chain ($C_{18:1}$, $C_{20:1}$, $C_{20:4}$) ceramides but not any other ceramides as substrates.[4] These results suggest that the three human alkaline ceramidases have distinct substrate specificity although they share a high degree of similarity in protein sequence. ACER2 also differs in the substrate specificity from the acid ceramidase, which prefers ceramides with medium acyl chains (20). The rat and human neutral ceramidases were shown to use ceramides with saturated or unsaturated long and very long acyl groups as substrates (21–23), suggesting that among the known ceramidases, ACER2 is closest in substrate specificity to the neutral ceramidase. Interestingly, it is noteworthy that ACER2 does not hydrolyze D-e-C_{12}-NBD-ceramide, a good substrate for the neutral ceramidase ASAH2 (23). Therefore, ACER2 activity can be distinguished from ASAH2 activity by using this synthetic ceramide analogue as substrate.

In vitro ACER2 activity is markedly increased by Ca^{2+} but not by other divalent cations, suggesting that ACER2 specifically requires Ca^{2+} for its optimal *in vitro* activity. We demonstrated that ACER2 overexpression caused a substantial increase in the levels of SPH in resting HeLa cells, indicating that ACER2 is constitutively activated by intracellular Ca^{2+}. As ACER2 is a transmembrane Golgi protein, it can be activated by Ca^{2+} either in the cytosol or in the lumen of the Golgi complex. We showed that the depletion of Ca^{2+} from the cytosol by BAPTA-AM only slightly inhibited the ACER2-catalyzed generation of SPH in cells, suggesting that free cytosolic Ca^{2+} is not required for ACER2 cellular activity. In contrast, treatment with THAP, which has been shown to decrease $[Ca^{2+}]_g$ (17), nearly abolished the ability of ACER2 to generate SPH in cells. Although THAP also decreases $[Ca^{2+}]$ in other intracellular Ca^{2+} stores, such as the ER, its inhibitory effect on ACER2 cellular activity appears to be linked to a decrease in $[Ca^{2+}]_g$ rather than other effects. This notion is supported by several lines of evidence. First, treatment with THAP increased rather than decreased ceramides in ACER2-TET-ON cells, suggesting that THAP does not inhibit the biosynthesis of ceramides. Second, ceramides are transported from the ER to the Golgi complex where they are incorporated into sphingomyelins. This process was not affected by THAP treatment because we demonstrated that treatment with THAP increased rather than decreased the levels of sphingomyelins. Third, we found that treatment with THAP did not alter the cellular localization of ACER2. These results suggest that the THAP-induced decrease in $[Ca^{2+}]_g$ attenuates the ACER2-mediated generation of SPH directly by inhibiting cellular ACER2 activity rather than by depleting its cellular substrates or altering its cellular localization. Based on these observations, we conclude that ACER2 requires Ca^{2+} in the lumen of the Golgi complex for its cellular activity.

Protein sequence analysis does not reveal a known Ca^{2+}-binding motif in ACER2, suggesting that ACER2 may have a novel Ca^{2+}-binding motif. Unlike other conventional Ca^{2+}-binding proteins or enzymes, ACER2 requires a relatively high $[Ca^{2+}]$ for its activity, suggesting that this novel Ca^{2+}-binding motif, if exists, may bind to Ca^{2+} with a high dissociation constant (K_d). $[Ca^{2+}]_g$ is ~300 μM in resting HeLa cells (24). We

[4] Hu, W., Xu, R., Sun, W., Szulc, Z. M., Bielawski, J., Obeid, L. M., and Mao, C. (2010) *J. Biol. Chem.* **285,** 7964–7976.

demonstrated that Ca^{2+} at this concentration maximally activated *in vitro* ACER2 activity, suggesting that Golgi Ca^{2+} fully activates ACER2 in resting cells. If this hypothesis is correct, cellular ACER2 activity is likely inhibited by stimuli or genetic conditions that decrease $[Ca^{2+}]_g$. Mutations of the secretory pathway Ca^{2+}-ATPase 1 (SPCA1/ATP2C1) decrease $[Ca^{2+}]_g$ in epidermal keratinocytes, the major cell type of the epidermis, and causes Hailey-Hailey disease manifested by the formation of painful blisters on the skin (25). With reverse transcription-PCR analysis, we demonstrated that ACER2 is expressed in the epidermis (data not shown). It is interesting to know whether ACER2 activity is inhibited in patients with Hailey-Hailey disease (benign familial pemphigus), and if so, whether ACER2 inhibition contributes to the symptom development of the disease.

As mentioned earlier, ACER2 has 7 putative TMDs. Consistent with the finding of an odd TMD number, we demonstrated that the N and C termini are oppositely oriented in the Golgi lumen and cytosol, respectively. The ACER2 mutant lacking the entire luminal N-terminal tail (the first 36 amino acids) was mainly localized to the ER rather than the Golgi complex, suggesting that the N-terminal tail is important for targeting of ACER2 to the Golgi complex. The ACER2 mutant is localized mainly to the ER, suggesting that ACER2 has an ER retrieval signal in a region outside the N-terminal tail. In the wild-type ACER2, this ER retrieval signal may be quenched by a Golgi targeting signal residing in the N-terminal tail, thus, it is correctly targeted to the Golgi complex. The Golgi targeting signal must reside in the region between the first and 13th amino acid residues because deletion of the first 13 amino acid residues at the N terminus renders ACER2 translocation from the Golgi complex to the ER. This region is distinct in amino acid sequence from the corresponding region of ACER1, an ER alkaline ceramidase that shares a high similarity in overall protein sequence to ACER2, further supporting the importance of this region in Golgi targeting. However, whether this region is sufficient for ACER2 to target to the Golgi complex is currently unknown. Studies on the Golgi targeting of membrane-bound proteins with a single TMD demonstrated that Golgi targeting can be determined by the length and composition of the TMD or a signal sequence(s) in various regions including the cytoplasmic N terminus, the combined cytoplasmic terminus and TMD, or luminal regions (26). Luo *et al.* (27) demonstrated that deleting the N-terminal tail or C-terminal tail, or replacing some of inter-TMD cytosolic or luminal loops of progesterone and adipoQ receptor 3, PAQR3 with 7 TMDs, also known as RKTG (Raf kinase trapping to Golgi), abolishes its localization to the Golgi complex. These observations suggest that multiple structural determinants are required for Golgi targeting of proteins with single TMD or multiple TMDs. This rule may also apply to ACER2.

We demonstrated that the ACER2 mutant lacking the first 36 amino acid residues had undetectable alkaline ceramidase activity, whereas the ACER2 mutant lacking the first 13 amino acid residues remains active, suggesting that the region between the 14th and 36th amino acid residues is critical for ACER2 activity. Sequence alignment reveals that this region is highly conserved among known alkaline ceramidases, suggesting that this region in other alkaline ceramidases may also be critical for their activities. In addition to the N-terminal tail, the three putative luminal loops are highly conversed among all alkaline ceramidases, whereas the C terminus and three putative cytosolic loops are much less or not conserved at all (6). This suggests that the active site of ACER2 may be located in the lumen of the Golgi complex. This view is in line with the finding that ACER2 is activated by Ca^{2+} in the Golgi lumen but not in the cytosol. The N-terminal tail of ACER2 may contain part or the whole active site of the enzyme, so its deletion renders ACER2 inactive. Based on these observations, we conclude that ACER2 catalyzes the hydrolysis of ceramides to generate SPH likely in the Golgi lumen.

Cellular localization is important for proteins or enzymes to exert their biological function. Our data suggest that mistargeting of ACER2 affects some of its biological roles. We previously demonstrated that SPH generated by ACER2 in the Golgi complex inhibits glycosylation of the β1 integrin subunit (19). In this study, we found that ACER2 overexpression also inhibited glycosylation of Lamp1, a highly glycosylated lysosomal protein, thus resulting in a shift of electrophoretic mobility. These results suggest that SPH generated by ACER2 in the Golgi complex has a general inhibitory effect on protein glycosylation. To our knowledge, SPH is the first endogenous bioactive lipid that inhibits protein glycosylation specifically in the Golgi complex. In contrast to SPH generated in the Golgi complex, SPH generated by the enzymatically active mutant ACER2ΔN13 in the ER failed to inhibit glycosylation of the integrin β1 subunit or Lamp1, suggesting that Golgi targeting of ACER2 is necessary for its ability to regulate protein glycosylation in the Golgi complex. This finding is in line with our previous study showing that SPH generated in the ER by overexpression of ACER1, an ER ceramidase, fails to inhibit glycosylation of the integrin β1 subunit in the Golgi complex (7). These two studies also clearly suggest that SPH generated in the ER cannot be transported in the free form to the Golgi complex.

We previously demonstrated that ACER2 has the ability to regulate cell proliferation mediated by S1P and its receptors. Our finding that overexpression of ACER2 in Golgi complex or its active mutant in the ER increased the levels of extracellular S1P, suggests that S1P generated from SPH either in the Golgi complex or the ER is secreted extracellularly. Therefore, mislocalization of ACER2 does not abolish its ability to control the release of S1P from cells. It is noteworthy that ACER2 mislocalization may quantitatively affect S1P release because ACER2 may produce SPH, the S1P precursor, to different levels in the ER and Golgi complex due to differences in the availability of its substrates in these two organelles. The current study with transient transfection cannot address this issue because the expression levels of ACER2 and its mutant were different.

In conclusion, we demonstrated that ACER2 has broad substrate specificity. Consistent with its *in vitro* activity, ACER2 catalyzes the hydrolysis of various cellular ceramides. ACER2 has an odd number of TMDs, and its N and C termini are oriented in the Golgi lumen and cytosol, respectively. The N terminus is essential for ACER2 activity, Golgi localization, and certain biological functions. ACER2 requires Ca^{2+} for its optimal activity both *in vitro* and in cells. Luminal Ca^{2+} is required

for the catabolism of sphingolipids by activating ACER2 in cells, suggesting that ACER2 may mediate Ca^{2+}-induced cellular responses.

Acknowledgment—We thank Dr. Jennifer Schnellmann for English proofreading and editing of the manuscript.

REFERENCES

1. el Bawab, S., Mao, C., Obeid, L. M., and Hannun, Y. A. (2002) *Subcell. Biochem.* **36,** 187–205
2. Maceyka, M., Milstien, S., and Spiegel, S. (2005) *Prostaglandins Other Lipid Mediat.* **77,** 15–22
3. Hannun, Y. A., and Obeid, L. M. (2002) *J. Biol. Chem.* **277,** 25847–25850
4. Cuvillier, O. (2002) *Biochim. Biophys. Acta* **1585,** 153–162
5. Spiegel, S. (1999) *J. Leukocyte Biol.* **65,** 341–344
6. Xu, R., Jin, J., Hu, W., Sun, W., Bielawski, J., Szulc, Z., Taha, T., Obeid, L. M., and Mao, C. (2006) *FASEB J.* **20,** 1813–1825
7. Sun, W., Hu, W., Xu, R., Jin, J., Szulc, Z. M., Zhang, G., Galadari, S. H., Obeid, L. M., and Mao, C. (2009) *FASEB J.* **23,** 658–666
8. Mao, C., Xu, R., Szulc, Z. M., Bielawska, A., Galadari, S. H., and Obeid, L. M. (2001) *J. Biol. Chem.* **276,** 26577–26588
9. Mao, C., Xu, R., Bielawska, A., Szulc, Z. M., and Obeid, L. M. (2000) *J. Biol. Chem.* **275,** 31369–31378
10. Mao, C., Xu, R., Bielawska, A., and Obeid, L. M. (2000) *J. Biol. Chem.* **275,** 6876–6884
11. Eckhardt, M., Gotza, B., and Gerardy-Schahn, R. (1999) *J. Biol. Chem.* **274,** 8779–8787
12. Bligh, E. G., and Dyer, W. J. (1959) *Can. J. Biochem. Physiol.* **37,** 911–917
13. Merrill, A. H., Jr., Wang, E., Mullins, R. E., Jamison, W. C., Nimkar, S., and Liotta, D. C. (1988) *Anal. Biochem.* **171,** 373–381
14. Van Veldhoven, P. P., and Bell, R. M. (1988) *Biochim. Biophys. Acta* **959,** 185–196
15. Bielawski, J., Szulc, Z. M., Hannun, Y. A., and Bielawska, A. (2006) *Methods* **39,** 82–91
16. Sun, W., Xu, R., Hu, W., Jin, J., Crellin, H. A., Bielawski, J., Szulc, Z. M., Thiers, B. H., Obeid, L. M., and Mao, C. (2008) *J. Invest. Dermatol.* **128,** 389–397
17. Van Baelen, K., Vanoevelen, J., Callewaert, G., Parys, J. B., De Smedt, H., Raeymaekers, L., Rizzuto, R., Missiaen, L., and Wuytack, F. (2003) *Biochem. Biophys. Res. Commun.* **306,** 430–436
18. Lin, P., Yao, Y., Hofmeister, R., Tsien, R. Y., and Farquhar, M. G. (1999) *J. Cell Biol.* **145,** 279–289
19. Sun, W., Hu, W., Xu, R., Jin, J., Szulc, Z. M., Zhang, G., Galadari, S. H., Obeid, L. M., and Mao, C. (2009) *FASEB J.* **23,** 656–666
20. Koch, J., Gärtner, S., Li, C. M., Quintern, L. E., Bernardo, K., Levran, O., Schnabel, D., Desnick, R. J., Schuchman, E. H., and Sandhoff, K. (1996) *J. Biol. Chem.* **271,** 33110–33115
21. El Bawab, S., Roddy, P., Qian, T., Bielawska, A., Lemasters, J. J., and Hannun, Y. A. (2000) *J. Biol. Chem.* **275,** 21508–21513
22. Usta, J., El Bawab, S., Roddy, P., Szulc, Z. M., Yusuf, Hannun, A., and Bielawska, A. (2001) *Biochemistry* **40,** 9657–9668
23. El Bawab, S., Usta, J., Roddy, P., Szulc, Z. M., Bielawska, A., and Hannun, Y. A. (2002) *J. Lipid Res.* **43,** 141–148
24. Pinton, P., Pozzan, T., and Rizzuto, R. (1998) *EMBO J.* **17,** 5298–5308
25. Hu, Z., Bonifas, J. M., Beech, J., Bench, G., Shigihara, T., Ogawa, H., Ikeda, S., Mauro, T., and Epstein, E. H., Jr. (2000) *Nat. Genet.* **24,** 61–65
26. van Dijk, A. D., Bosch, D., ter Braak, C. J., van der Krol, A. R., and van Ham, R. C. (2008) *Bioinformatics* **24,** 1779–1786
27. Luo, X., Feng, L., Jiang, X., Xiao, F., Wang, Z., Feng, G. S., and Chen, Y. (2008) *Biochem. J.* **414,** 399–406